

PROCEEDINGS OF THE

**SIXTH CANADIAN MARINE
HYDROMECHANICS AND STRUCTURES
CONFERENCE**

23-26 May, 2001
Vancouver, BC

© The Sixth Canadian Marine Hydromechanics and Structures
Conference
Professor S. M. Calisal
Department of Mechanical Engineering
University of British Columbia
2324 Main Mall
Vancouver, BC
V6T 1Z4 Canada
calisal@mech.ubc.ca

A NONLINEAR DISPERSIVE WAVE MODEL FOR WAVE PROPAGATION IN IRREGULAR DOMAINS

Serdar BEJI¹ and Barış BARLAS¹

ABSTRACT

A recently introduced wave model (Nadaoka *et. al.*, 1997) is re-expressed in boundary fitted non-orthogonal curvilinear co-ordinate system for simulating wave motions in domains with irregular boundaries. The co-ordinate transformation converts an irregular physical domain into a rectangular computational domain. The boundary conditions for irregular vertical enclosures surrounding a typical physical domain, such as a channel, port or harbour, are satisfied accurately. Comparisons of computational results with experimental measurements and various cases for simulating waves inside harbours and channels show good agreement and establish confidence for practical applications of the model developed.

1. MATHEMATICAL FORMULATION

The wave model adopted in this work is the single-component form of the fully-dispersive weakly-nonlinear wave equations of Nadaoka *et. al.* (1997). The wave model is valid for arbitrary depths, ranging from infinitely deep to very shallow waters. The model is thus capable of simulating the second-order Stokes waves and cnoidal waves equally well. The continuity and momentum equations of the wave model are given as

$$\frac{\partial \zeta}{\partial t} + \nabla \cdot \left[\left(\frac{C_p^2}{g} + \zeta \right) \bar{u} \right] = 0, \quad (1)$$

$$\begin{aligned} & C_p C_g \frac{\partial \bar{u}}{\partial t} + \\ & C_p^2 \nabla \left[g \zeta + \zeta \frac{\partial w}{\partial t} + \frac{1}{2} (\bar{u} \cdot \bar{u} + w^2) \right] \\ & = \frac{\partial}{\partial t} \left[\frac{C_p (C_p - C_g)}{k^2} \nabla (\nabla \cdot \bar{u}) \right] \\ & + \nabla \left[\frac{C_p (C_p - C_g)}{k^2} \right] (\nabla \cdot \bar{u}) \end{aligned} \quad (2)$$

where \bar{u} is the horizontal velocity vector and w the vertical component of velocity both at $z=0$. ζ is the free surface elevation, h the local water depth as measured from the still water level, and ∇ the horizontal gradient operator with $(\partial/\partial x, \partial/\partial y)$ components. C_p , C_g , and k denote respectively the phase and group velocities and wave number, computed according to the linear theory for a prescribed dominant frequency ω and a given local depth h .

1.1. Transformed Wave Equations

The boundary fitted curvilinear co-ordinate system (ξ, η) , sketched in Figure 1, is now introduced. Here, ξ is taken usually (not necessarily) in the direction of wave propagation while η is taken perpendicular to the ξ lines.

The wave equations are transformed from the physical space (x, y) to the computational space (ξ, η) by the following co-ordinate transformation relations (Hoffman and Chiang, 1995):

¹ Dept. of Naval Architecture and Ocean Engineering, Istanbul Technical University, Maslak 80626, Istanbul, Turkey

$$\begin{aligned} \tau = t, \quad \xi = \xi(t, x, y), \quad \eta = \eta(t, x, y) \\ \frac{\partial}{\partial t} = \frac{\partial}{\partial \tau}, \quad \frac{\partial}{\partial x} = \xi_x \frac{\partial}{\partial \xi} + \eta_x \frac{\partial}{\partial \eta}, \\ \frac{\partial}{\partial y} = \xi_y \frac{\partial}{\partial \xi} + \eta_y \frac{\partial}{\partial \eta} \end{aligned} \quad (3)$$

The continuity (1) and momentum equations (2) are re-expressed in curvilinear non-orthogonal co-ordinates using the above transformations. However, the Cartesian velocity components are not transformed hence the components of the momentum equation are still in Cartesian directions. This results in a formulation with less metric coefficients in the transformed equations, which read

$$\begin{aligned} \frac{\partial \zeta}{\partial \tau} + \xi_x \frac{\partial P}{\partial \xi} + \eta_x \frac{\partial P}{\partial \eta} \\ + \xi_y \frac{\partial Q}{\partial \xi} + \eta_y \frac{\partial Q}{\partial \eta} = 0 \end{aligned} \quad (4)$$

for continuity, and

$$\begin{aligned} C \cdot \xi_x^2 \frac{\partial^3 u}{\partial \xi^2 \partial \tau} + CX \cdot \xi_x \frac{\partial^2 u}{\partial \xi \partial \tau} \\ - R \cdot \frac{\partial u}{\partial \tau} = RH_x \end{aligned} \quad (5)$$

$$\begin{aligned} C \cdot \eta_y^2 \frac{\partial^3 v}{\partial \eta^2 \partial \tau} + CY \cdot \eta_y \frac{\partial^2 v}{\partial \eta \partial \tau} \\ - R \cdot \frac{\partial v}{\partial \tau} = RH_y \end{aligned} \quad (6)$$

for x- and y- momentum equations, respectively. Here, u, v are the velocity components at the still water level in the Cartesian coordinates. P, Q, R, C, CX, CY, RH_x, and RH_y are defined as

$$C = \frac{C_p^2(1-R)}{\omega^2} \quad (7a)$$

$$CX = \frac{1}{\omega^2} \left(\begin{aligned} &\xi_x \frac{\partial}{\partial \xi} (C_p^2(1-R)) \\ &+ \eta_x \frac{\partial}{\partial \eta} (C_p^2(1-R)) \end{aligned} \right) \quad (7b)$$

$$CY = \frac{1}{\omega^2} \left(\begin{aligned} &\xi_y \frac{\partial}{\partial \xi} (C_p^2(1-R)) \\ &+ \eta_y \frac{\partial}{\partial \eta} (C_p^2(1-R)) \end{aligned} \right) \quad (7c)$$

$$P = \left(\frac{C_p^2}{g} + \zeta \right) \cdot u \quad Q = \left(\frac{C_p^2}{g} + \zeta \right) \cdot v \quad R = \frac{C_g}{C_p} \quad (7d)$$

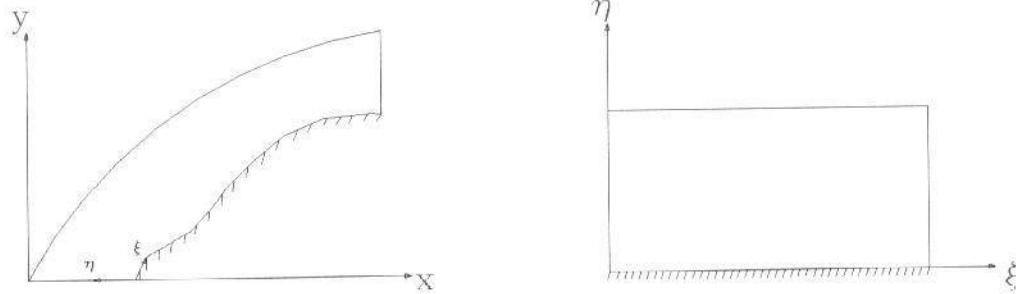


Figure 1. A sketch representing co-ordinate transformation from the physical domain to the computational domain.

$$\begin{aligned}
RH_x &= \xi_x \frac{\partial S}{\partial \xi} + \eta_x \frac{\partial S}{\partial \eta} \\
&- C \cdot \left(\begin{aligned} &\xi_{xy} \frac{\partial^2 v}{\partial \tau \partial \xi} + \eta_{xy} \frac{\partial^2 v}{\partial \tau \partial \eta} \\ &+ \xi_x \xi_y \frac{\partial^3 v}{\partial \tau \partial \xi^2} + \eta_x \eta_y \frac{\partial^3 v}{\partial \tau \partial \eta^2} \\ &+ \xi_x \eta_y \frac{\partial^3 v}{\partial \tau \partial \xi \partial \eta} + \eta_x \xi_y \frac{\partial^3 v}{\partial \tau \partial \xi \partial \eta} \end{aligned} \right) \\
&- C \cdot \left(\begin{aligned} &\eta_x^2 \frac{\partial^3 u}{\partial \tau \partial \eta^2} + 2\xi_x \eta_x \frac{\partial^3 u}{\partial \tau \partial \xi \partial \eta} \\ &+ \xi_{xx} \frac{\partial^2 u}{\partial \tau \partial \xi} + \eta_{xx} \frac{\partial^2 u}{\partial \tau \partial \eta} \end{aligned} \right) \\
&- CX \cdot \left(\begin{aligned} &\xi_y \frac{\partial^2 v}{\partial \tau \partial \xi} + \eta_y \frac{\partial^2 v}{\partial \tau \partial \eta} \\ &+ \eta_x \frac{\partial^2 u}{\partial \tau \partial \eta} \end{aligned} \right)
\end{aligned} \tag{8a}$$

$$\begin{aligned}
RH_y &= \xi_y \frac{\partial S}{\partial \xi} + \eta_y \frac{\partial S}{\partial \eta} \\
&- C \cdot \left(\begin{aligned} &\xi_{xy} \frac{\partial^2 u}{\partial \tau \partial \xi} + \eta_{xy} \frac{\partial^2 u}{\partial \tau \partial \eta} \\ &+ \xi_x \xi_y \frac{\partial^3 u}{\partial \tau \partial \xi^2} + \eta_x \eta_y \frac{\partial^3 u}{\partial \tau \partial \eta^2} \\ &+ \xi_x \eta_y \frac{\partial^3 u}{\partial \tau \partial \xi \partial \eta} + \eta_x \xi_y \frac{\partial^3 u}{\partial \tau \partial \xi \partial \eta} \end{aligned} \right) \\
&- C \cdot \left(\begin{aligned} &\eta_x^2 \frac{\partial^3 v}{\partial \tau \partial \eta^2} + 2\xi_x \eta_x \frac{\partial^3 v}{\partial \tau \partial \xi \partial \eta} \\ &+ \xi_{xx} \frac{\partial^2 v}{\partial \tau \partial \xi} + \eta_{xx} \frac{\partial^2 v}{\partial \tau \partial \eta} \end{aligned} \right) \\
&- CY \cdot \left(\begin{aligned} &\xi_x \frac{\partial^2 u}{\partial \tau \partial \xi} + \eta_x \frac{\partial^2 u}{\partial \tau \partial \eta} \\ &+ \eta_y \frac{\partial^2 v}{\partial \tau \partial \eta} \end{aligned} \right)
\end{aligned} \tag{8b}$$

ξ_x, ξ_y, \dots appearing in equations (3)-(8) are the grid metrics, and S is given by

$$S = g \cdot \zeta + \zeta \frac{\partial w}{\partial \tau} + \frac{1}{2} (u^2 + v^2 + w^2) \tag{9}$$

2. NUMERICAL APPROACH

The transformed continuity and momentum equations (4-5-6) are discretized by finite difference approximations using non-staggered grids, where the free surface displacement, the velocity

components, and the grid metrics are defined at the grid intersections. The second-order central-difference formulae are used for approximating all the partial derivatives both in time and space. The basic algorithm is divided into two stages: In the first stage, the velocity components are computed by solving the momentum equations (5-6) until a specific convergence criterion is met. The solution of the velocity components requires the use of Thomas algorithm, which is quite efficient in the solution of tridiagonal matrix systems. Then, using the final velocity components, the free surface elevation is obtained from the continuity equation (4) at each time step.

The boundary conditions on the free surface and on the bottom are automatically satisfied by the wave equations. It then remains to specify the conditions on the incident and outgoing boundary and on the vertical enclosures surrounding the domain. The conditions at the incoming boundary are easily specified by introducing an incident wave field; likewise, the wall condition, which states that the velocity normal to the wall surface must vanish, is satisfied easily in the transformed rectangular computational domain. The radiation condition usually presents difficulties since there is no perfect radiation condition for nonlinear directional waves leaving the domain. Here, the second-order radiation condition of Engquist and Majda (1977) is used to minimise the artificially reflected waves from the outgoing boundary.

2.1. Wave Propagation Over a Topographical Lens

A sample computation using the above scheme for the case of wave propagation over a topographical lens (Whalin, 1972) is performed. The bathymetry is given by

$$h(x, y) = \begin{cases} 0.4572; & 0 \leq x < 10.7 - G \\ 0.4572 + (10.7 - G - x)/25; & 10.67 - G \leq x < 18.3 - G \\ 0.1524; & 18.3 - G \leq x \leq 21.3 \end{cases} \tag{10}$$

where

$$G(y) = [y(6.096 - y)]^2 \text{ for } 0 \leq y \leq 6.096$$

Figure 2 shows the bathymetry according to these definitions.

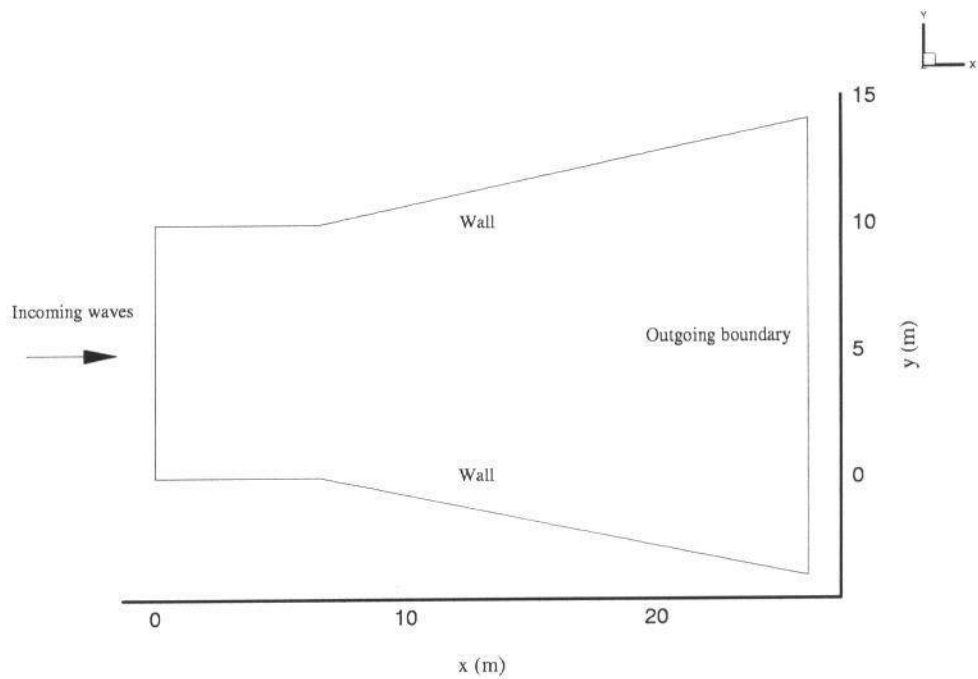


Figure 5. Channel geometry used for simulating waves in a widening channel.

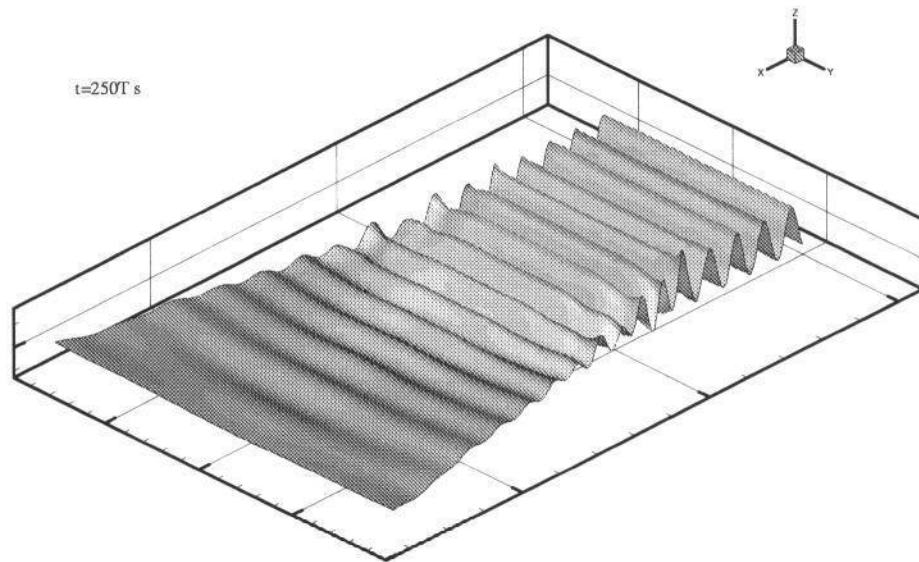


Figure 6. Time domain simulation of the wave field in a diverging channel

3. Concluding Remarks

The recently developed nonlinear wave model of Nadaoka *et al.* (1997) has been re-expressed in the boundary fitted curvilinear co-ordinate system to achieve accurate treatment of the boundary conditions for irregular physical domains. The numerical scheme based on the transformed wave equations is first used for a sample simulation of nonlinear wave propagation over a topographical

lens and the results are found to be quite acceptable. Furthermore, time domain simulations of sinusoidal regular waves entering a marina are given to illustrate typical diffraction patterns. Finally, numerical simulation of wave propagation in a diverging channel is presented. Thus, it may be concluded that the model introduced here shows promising aspects for future practical applications, especially in the simulations of waves in domains with arbitrary boundaries.

References

ENGQUIST, B. and MAJDA, A. (1977). Absorbing boundary conditions for the numerical simulation of waves. *Math. Comp.* **31**, 1977, 629-651.

HOFFMANN, K.A. and CHIANG, S.T. *Computational Fluid Dynamics for Engineers – Volume: 1, 2*, Engineering Education System Publication, Wichita, 1995.

NADAOKA, K., BEJI, S. and NAKAGAWA, Y. (1997). A fully dispersive weakly nonlinear model for water waves, *Proc. Royal Soc., London, Ser A*, **453**, 303-308.

WHALIN, R.W. *The Limit of Applicability of Linear Refraction Theory in a Convergence Zone*. Res. Rep. H-71-3, U.S. Army Corps of Engrs., Waterways Expt. Station, Vicksburg, M.S., 1971.